English
Summary Ph.D. thesis

Window Cooling for Solar High-Temperature Receivers

Fensterkühlung für solare Hochtemperatur-Receiver

Marc Röger

Deutsches Zentrum für Luft- und Raumfahrt
Institut für Technische Thermodynamik

Please cite with:
Röger, Marc, Fensterkühlung für solare Hochtemperatur-Receiver. Fortschritt-Berichte VDI 6, no. 534, VDI Verlag, Düsseldorf, 2005, ISBN 3-18-353406-1

DLR Deutsches Zentrum für Luft- und Raumfahrt e.V.
in der Helmholtz-Gemeinschaft

Overview

Who remains on the coast,
cannot discover new oceans.

F. Magellan

1 Introducing Remarks

This is a short English summary of the Ph.D. thesis written in German. The summary section chapters are corresponding to the Ph.D. thesis. Large parts of the thesis have also been published in international journals. To get detailed information in English, you may read the publications [1]-[3] listed on the right-hand side.

The Ph.D. thesis is dealing with an air-jet cooling of a solar receiver window. Great part of the research done is important to thermal science and heat transfer and may be applied to other applications.

Fig. 1 gives an overview of the thesis structure. First, a thermodynamic receiver model to calculate window heat flows and temperatures was developed (section 3, Paper [3]). Knowing the required cooling fluxes and distribution on the window surface, various external air-jet window cooling systems were designed (section 4, Paper [1]) and flow and heat transfer of different air-jet cooling configurations were studied numerically (section 5, Paper [1]). The heat transfer coefficient was measured in high resolution on the two-dimensional curved window surface to validate the CFD calculations. For this, a periodic transient heat transfer measurement technique was further developed into an accurate high-resolution measurement technique. The patented work on the periodic measurement technique can be considered as one of the main issues of the Ph.D. thesis (section 6, Paper [2]). By means of the measurements, the simulations could be validated and correlations for different air-jet window cooling configurations were derived. It is shown that the best configuration is an asymmetric pulsating air-jet cooling (section 7, Paper [1]). Finally, the thermodynamic receiver model of section 3 and the proper working of the air-jet cooling was validated by solar field test measurements (section 8, Paper [3]).

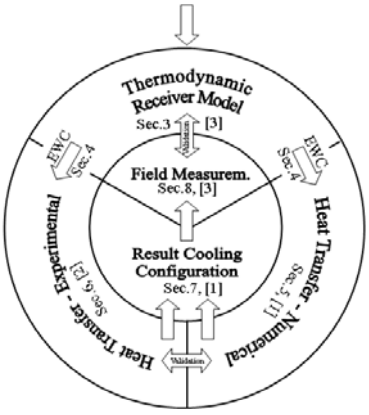

Fig. 1: Overview of PhD thesis (EWC=External Window Cooling)

[1] RÖGER, M.; BUCK, R.; MÜLLER-STEINHAGEN, H.: *Numerical and Experimental Investigation of a Multiple Air Jet Cooling System for Application in a Solar Thermal Receiver.* J. Heat Transfer, Vol. 127, No. 8, 2005, pp. 863-876.

[2] RÖGER, M.: *A Periodic Transient Method for High-Resolution Heat Transfer Measurement on Two-Dimensional Curved Surfaces.* To be published in J. Heat Transfer, Assigned to Issue Dec 2007.

[3] RÖGER, M.; PFÄNDER, M.; BUCK, R.: *Multiple Air-Jet Window Cooling for High-Temperature Pressurized Volumetric Receivers: Testing, Evaluation, and Modeling*. J. Sol. Energy Eng., Vol. 128, No. 3, 2006, pp. 265-274.

2 Introduction and Objective

One path to convert solar radiation into electricity is to supply solar heat to a thermodynamic cycle. This is done by concentrating solar radiation onto a receiver, which absorbs the radiant energy and heats a heat transfer medium (see Fig. 2).

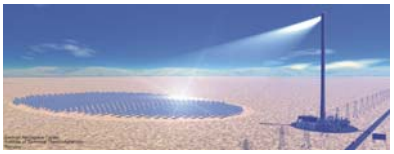

Fig. 2: Artistic view of a solar tower plant (40 MW_{el})

In central receiver technology, high solar concentration factors between 200 and 1000 enable high working temperatures and the integration of solar energy into the topping Brayton cycle of a combined cycle. Hence, solar energy can be converted highly efficient to electricity. The concept of solar air preheating for gas turbines is shown in Fig. 3.

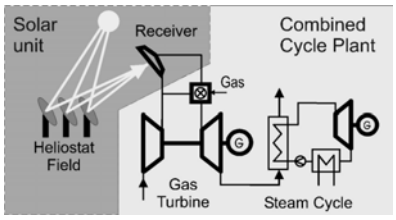

Fig. 3: Solar air heating system for a combined cycle

Compressed air is heated efficiently by a pressurized volumetric solar receiver, shown in Fig. 4. The receiver module consists mainly of an insulated pressure vessel, covered by a concave fused-silica window. Concentrated sunlight goes through the secondary concentrator and the fused-silica window and then is absorbed in the volumetric absorber which heats the compressed air.

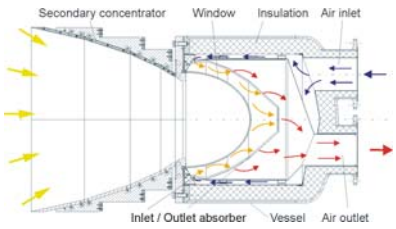

Fig. 4: Pressurized volumetric receiver

High air outlet temperatures increase the solar share of pressurized solar receivers for gas turbines, operated in solar-fossil hybrid mode. However, an increase in outlet temperature over 800°C leads to excessive heating of the receiver window, unless it is actively cooled.

This thesis solves the window overheating problem by designing and studying flow field and heat transfer of a multiple air-jet cooling. Nozzle positions typical in engineering could not be used because the nozzles must not block concentrated solar radiation. Conventional jet-cooling configurations with constant mass flows show too inhomogeneous heat transfer and poor cooling at the window top.

Both numerical and experimental methods were used for the investigation. A main issue of the thesis was the development of an accurate, high-resolution heat transfer measurement technique, which is suitable for measurements on two-dimensional curved surfaces. Stationary methods require the knowledge of accurate heat fluxes and temperatures which complicate measurements on curved surfaces. For the used periodic transient method, a procedure for the transient thermal characterization of the heating system was developed.

3 Thermodynamic Receiver Model

In order to properly predict window temperatures and receiver losses of a closed receiver, a thermodynamic receiver model was developed. Focus was on the fused-silica window. Various energy transport processes have to be considered: Solar radiation, thermal radiation, free or forced convection, and conduction.

A solar ray-tracing Monte-Carlo code was extended to calculate the absorbed solar radiation in the receiver window as a function of the incident angle, complex refractive index and glass thickness. Multiple reflections inside the glass volume were considered. The calculated absorbed solar radiation in the window was used as a source term in the discretized window elements.

The radiative heat transfer between the absorber, semi-transparent window and ambient is modeled by applying the enclosure method (zone method), which was introduced by Hottel. The non-gray spectral properties of fused silica were modeled by discretization of the radiative spectrum in different wavelength bands. Fig. 5 shows the spectral radiant fluxes of a window volume.

Convection is considered on both window inside and outside surface. Transversal heat transfer is a combination of conductive and radiant heat transfer inside the glass volume and is modeled by an effective thermal conduction.

The simulations showed that the highest heat input is caused by absorption of thermal radiation emitted by the absorber. For an enduring, safe operation, the window must be cooled actively for absorber temperatures higher than 820°C.

The thermodynamic receiver model is a viable tool for future designs of closed receivers with semi-transparent window. It predicts window temperatures, required heat transfer coefficients for active cooling systems (Fig. 6) and receiver losses for different operation conditions.

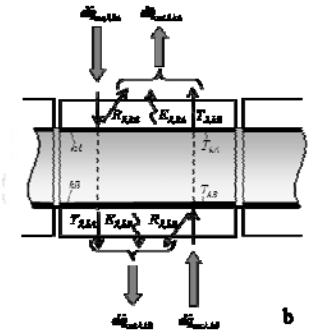

Fig. 5: Spectral radiant fluxes of surfaces *kA* and *kB*

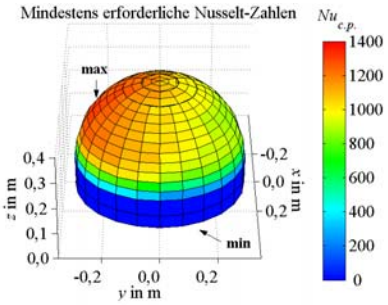

Fig. 6: Minimum required heat transfer for window temperatures below 800°C (absorber temperature 1000°C)

You may also see paper [3] for more details.

4 External Window Cooling

There are various requirements for a window cooling system. It must provide a sufficient heat transfer coefficient to keep window temperatures below 800°C while having low parasitic energy consumption. Furthermore, a more or less homogeneous temperature distribution to minimize thermal stresses is required. Finally, it has to comply with optical restraints.

External window cooling means that the receiver window is cooled by air jets impinging on the non-pressurized side. The air nozzles can only be positioned at the window bearing area in order to not block the incoming solar radiation. As a consequence, nozzle positions typical in engineering could not be used. The domed, cavity-like substrate also differs from cooling configurations commonly found in literature.

Fig. 7 to 9 show the examined cooling configurations. In all cases, the nozzles are distributed equally over the circumference of the window bearing area. Symmetric configurations supply all active nozzles with the same mass flow. To enhance and smooth out heat transfer distribution, symmetric configurations with several different swirled flows were also studied (Fig. 8). Finally, asymmetric configurations with pulsating mass flow were investigated (Fig. 9). In this configuration, nozzles are only active on one side of the window, while the others are deactivated. By sequentially switching nozzles on and off, the well-cooled region is moved around the circumference of the window.

Flow field and heat transfer of the examined configurations depend on a large number of variables. A dimensional analysis showed that the heat transfer at a point P depends on the following quantities:

Nu_P= f (Re, Pr, I, L_P/d_h, ϕ_P, T_w/T_f, n, ϕ_i, φ_i, ϑ_i) + nozzle type

Keeping this functional dependence in mind, the window-cooling designs were studied numerically (section 5) and experimentally (section 6).

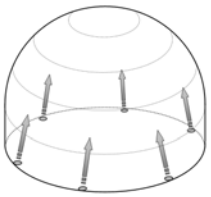

Fig. 7: Symmetric window-cooling design

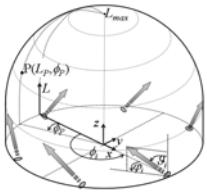

Fig. 8: Symmetric, swirled window-cooling design

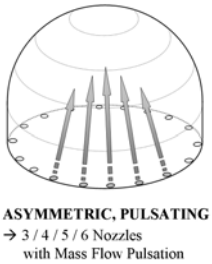

Fig. 9: Asymmetric, pulsating window-cooling design

You may also see paper [1] for more details.

5 Computational Fluid Dynamics

The CFD code FLUENT was used to calculate flow field and heat transfer on the receiver window. Simulations with the realizable k-ε model, SST-k-ω model and k-ω model were done in order to draw a comparison. The computational domain was discretized by a high-quality hybrid mesh down to the viscous sublayer. Fig. 10 shows the initial mesh and boundary conditions.

Iteration and discretization errors were evaluated. A grid refinement study was performed. It is concluded that the mean Nusselt number can be calculated with a discretization error of approximately 3.5% on the initial grid. In order to calculate grid-independent maximum Nusselt numbers, an adaptive grid refinement must be performed. With the adaptive refinement, the discretization error can be reduced to approximately 1%.

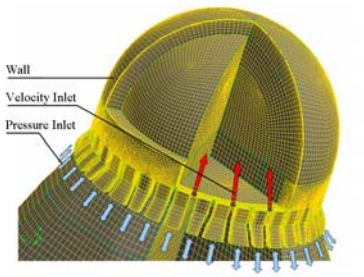

Fig. 10: Initial mesh and boundary conditions

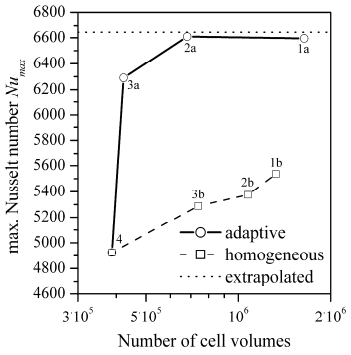

Fig. 11: Mesh refinement study

You may also see paper [1] for more details.

6 Heat Transfer Measurements

Heat transfer measurements and flow visualization experiments were done to validate the CFD calculations. A periodic transient heat transfer measurement technique was used, because it offers many advantages in the field of spatially resolved measurements, especially if applied to two-dimensional curved surfaces. In contrast to stationary methods, neither uniform heating of the measurement surface, nor quantitative determination of the substrate or fluid temperature is required. As a consequence, simpler heating devices can be used (homogeneous heat flux is not required) and time-consuming calibration of temperature sensors and thermography unit can be avoided without reducing measurement accuracy.

In the periodic transient method described, the substrate is excited by a sinusoidal modulated heat flux (see Fig. 12). The system along with its boundary conditions represents a continuous linear system with distributed parameters. It can be described by a partial differential equation of position and time. The system input is the penetrating heat flux on the heated side, the output is the measured temperature on the cooled side. Fig. 13 illustrates the Bode diagram for a 5-mm thick fused-silica hollow-sphere substrate. The heat transfer coefficient can be calculated by evaluating the phase shift between the penetrating heat flux and the resulting substrate temperature signal. Fig. 14 is a plot of the characteristic curves for heat transfer determination by phase response evaluation on a 5-mm thick fused-silica sphere. Analytical equations for both a flat-plate and a hollow-sphere substrate were derived.

In the Ph.D. thesis, the periodic transient measurement method was further developed into an accurate high-resolution measurement technique which can be used on two-dimensional curved surfaces. The proper operation of a simple, low-cost heating system made of commercial lamps (light bulbs) was demonstrated.

Due to the thermal inertia of the heating system and the substrate, the heat flux penetrating into the substrate is phase-shifted to the electric heating power.

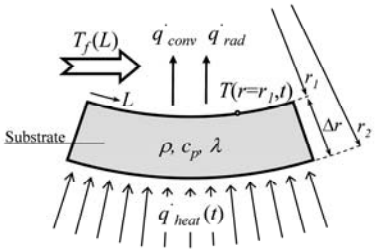

Fig. 12: Measurement principle and relevant quantities

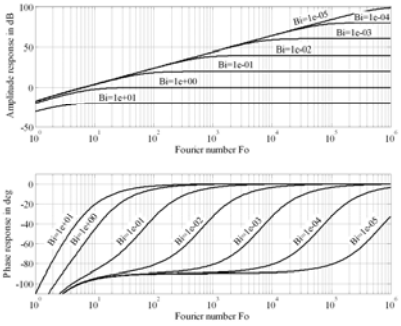

Fig. 13: Amplitude and phase response for different Bi numbers

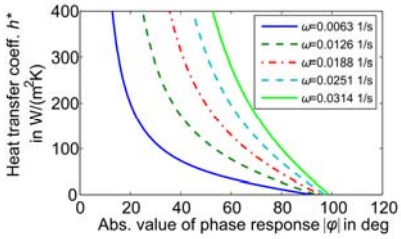

Fig. 14: Characteristic curves for heat transfer determination by phase response evaluation

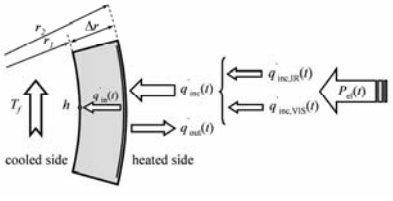

Fig. 15: Energy flows and heat fluxes on the window inside

You may also see paper [2] for more details.

This phase shift must not be neglected, as often done in literature, otherwise this leads to wide errors in heat transfer calculation. The conditions on the heated side are illustrated in Fig. 15. Fig. 16 shows the electric heating power, incident, outgoing and penetrating heat fluxes at two points with different heat transfer coefficient. The vertical lines point out the different phase angles.

A procedure for finding the transient penetrating heat flux signal from applied electric heating power by evaluating the measured surface temperature amplitude was developed and patented. The required penetrating heat flux is measured locally by a heat flux sensor. The surface temperature amplitude on the cooled side, which depends on the actual heat transfer coefficient, and the phase shift between the penetrating heat flux and the electric heating power are measured simultaneously. By repeating this procedure for different flow conditions, the characteristic heating curve shown in Fig. 17 can be plotted. This characterization is crucial for correct application of the method and need be done only once during measurement setup. Fig. 18 shows measurements of the electric heating power and temperature on the cooled side over time. The penetrating heat flux was calculated by using the correction phase shift of the heating characterization of Fig. 17.

Fig. 19 shows the measurement setup consisting of the forced-convection jet-cooling air supply and distribution systems, the domed fused-silica substrate, lamp heating, infrared thermography, and data acquisition systems. To ensure that the flow model emulates the real solar receiver, a secondary concentrator model was erected in front of the window. A rigorous uncertainty estimation was performed.

The periodic transient method described complements established techniques for high-resolution heat transfer measurements on two-dimensional curved surfaces. It is specially suitable for applications where a quantitative determination of the applied heat flux and the substrate or fluid temperatures result difficult.

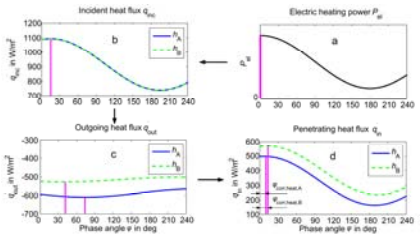

Fig. 16: Energy flows and heat fluxes over time

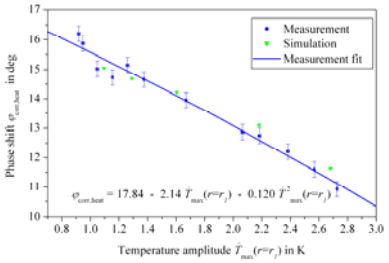

Fig. 17: Characteristic heating curve

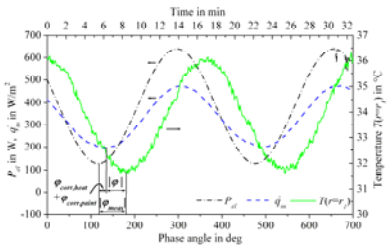

Fig. 18: Phase shift |φ| found from measured phase shift and correction phase shifts

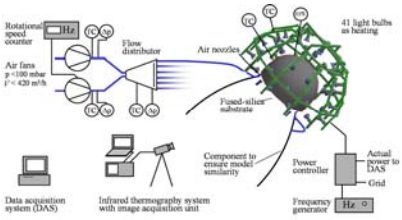

Fig. 19: Measurement setup

You may also see paper [2] for more details.

7 Simulation and Measurement Results

Fig. 20 shows measured and simulated heat transfer distributions for a symmetric air-jet cooling with six nozzles. For comparison, the simulations were performed with the realizable k-ε model, SST-k-ω model and k-ω model. The spreading of the jets is similar in measurement and the performed simulations. Also, the low heat transfer in the stagnation point at the top of the window is observed in measurement and simulations.

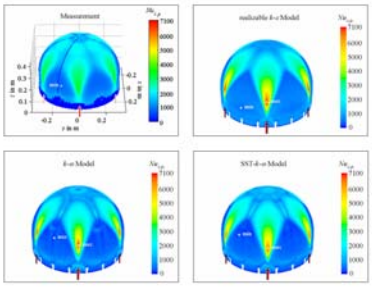

Fig. 20: Measured and simulated heat transfer, symmetric air-jet cooling with six nozzles

However, the maximum heat transfer values of the simulations of all turbulence models are much higher than the measured ones. This is clarified in Fig. 21, where the maximum experimental Nusselt number was corrected for lateral conduction. The error bars of the experiment both contain the measurement uncertainty, as the uncertainty in comparability. Comparing maximum Nusselt numbers, it strikes that the difference between calculated and measured values is higher than the error bars. This implies a modeling error. It is assumed that in the simulations, even though the spreading is predicted correctly, the models do not correctly describe turbulence structure and heat transfer near the impingement point. It is assumed that an excessive production of turbulent kinetic energy at the impingement point is responsible for the high heat transfer.

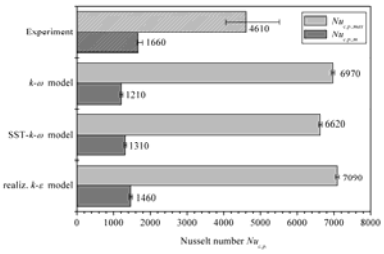

Fig. 21: Maximum and mean Nu number, symmetric air-jet cooling with six nozzles

In Fig. 21, also the mean heat transfer over the window surface is shown. Here, the deviation between simulations and experiment is smaller. The mean heat transfer calculated with the realizable k-ε model shows the best agreement with measurements.

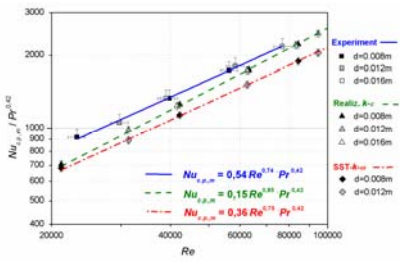

Fig. 22: Mean heat transfer on window surface, symmetric air-jet cooling with six nozzles

As expected, simulations and measurements indicate that only the flow field and heat transfer near the nozzles are influenced by the nozzle diameter. Measurements or simulations with the same Reynolds number produce the same mean heat transfer, regardless of nozzle dimension (see Fig. 22). Hence, the nozzle geometry can be fit to the limited available space at the receiver module, while maintaining the required heat transfer by simply adjusting the mass flow. The functional dependences of the mean heat transfer is shown in Fig. 22.

You may also see paper [1] for more details.

Measurements and simulations indicate that the symmetric non-swirled air-jet configurations cause high gradients in heat transfer near the jet impingement regions. This results in hot spots and high thermal stresses. One idea to enhance the heat transfer and homogenize the temperature distribution over the window surface is to generate a swirled flow in the window cavity. This is achieved by inclining the nozzles. Fig. 23 shows the resulting heat transfer distribution. The peaks with maximum heat transfer are lowered significantly. However, a vortex is generated with low velocities in the axis of symmetry, resulting in poor heat transfer at the top of the window.

As both the swirled and non-swirled symmetric air-jet cooling do not produce a homogeneous distribution of heat transfer on the window surface, an asymmetric configuration was considered. Fig. 24 shows the flow field with five simultaneously active nozzles. You can see that there is no stagnation point at the window top anymore. In Fig. 25, the measured heat transfer distribution is shown. The heat transfer at the window top is much higher than in the symmetric cases. However, while high Nusselt numbers can be observed at the impingement points, at both sides of the region of active nozzles, the heat transfer is only poor. A homogenization of the heat transfer distribution is achieved by periodic mass flow rate pulsation, i.e. nozzles are sequentially switched on and off so that the well-cooled region moves around the circumference of the window.

By means of the asymmetric, pulsating air-jet cooling, it is possible to homogenize the heat transfer distribution and generate the necessary heat fluxes at the top of the window, hence reducing high temperatures and temperature gradients.

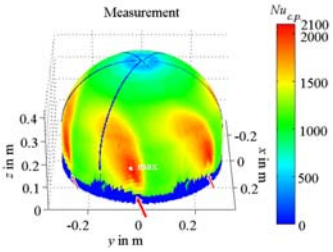

Fig. 23: Measured heat transfer, symmetric swirled air-jet cooling with six nozzles

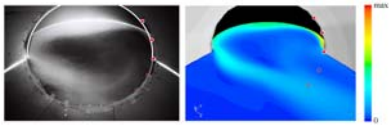

Fig. 24: Flow field with asymmetric configuration with five nozzles; visualization (left) and simulation (right)

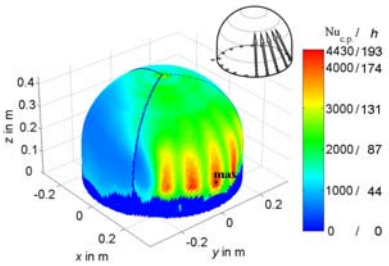

Fig. 25: Measured heat transfer, asymmetric, non-pulsating air-jet cooling (5 of 18 slot-type nozzles)

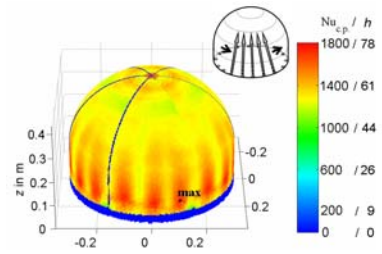

Fig. 26 Measured heat transfer, asymmetric, pulsating air-jet cooling (5 of 18 slot-type nozzles)

You may also see paper [1] for more details.

Fig. 27 shows the simulated temperature on the window inside at an absorber temperature of 1000°C and operating asymmetric pulsating air-jet cooling. The maximum fused silica temperature is below the required 800°C. Without active cooling, window temperature would have reached up to 940°C.

In Fig. 28, the mean heat transfer over the Reynolds number for different asymmetric cooling configurations with between three and six simultaneously active slot-type nozzles is shown. The necessary cooling flux can be adjusted to the actual operating conditions of the receiver by simply adapting the nozzle mass flow rate. You can also see that the more nozzles are simultaneously in operation, the lower the Reynolds number must be to achieve a certain mean heat transfer. In the Ph.D. thesis, it was shown that from an energetic point of view, configurations with five or six simultaneously operating nozzles are best.

Fig. 29 shows the blower power over the hydraulic diameter of the nozzle. The minimum power consumption is achieved by using nozzles with an hydraulic diameter of approximately 12.5 mm. Due to the limited space (optical reasons), slot-type nozzles were utilized. The parasitic power consumption lies in the order of 0.2% of the electricity produced. The cycle duration should be between 20 and 30 s.

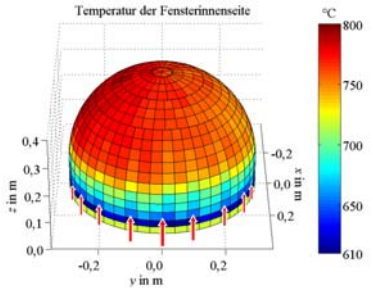

Fig. 27: Simulated temperature on the window inside, pulsating air-jet cooling (5 of 18 slot-type nozzles, absorber temp. 1000°C)

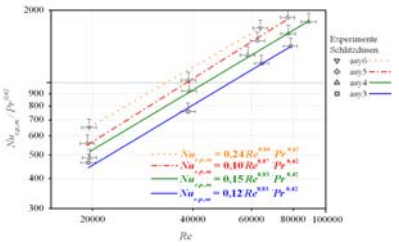

Fig. 28: Mean heat transfer on window surface, pulsating air-jet cooling (3/4/5/6 of 18 slot-type nozzles)

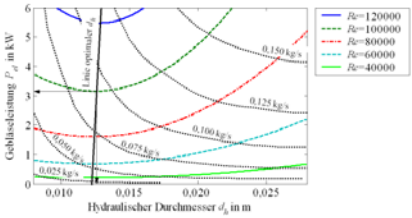

Fig. 29: Blower power over hydraulic nozzle diameter for different Re numbers, pulsating air-jet cooling with 5 of 18 nozzles

You may also see paper [1] for more details.

8 Solar Field Measurements

Solar field measurements at a high-temperature receiver module were performed at the Plataforma Solar de Almería. The test system comprising of three receiver modules and a solarized gas turbine provided up to 240 kW_{el}. The 18 preinstalled slot nozzles for the external window cooling system of the high-temperature module are shown in Fig. 30. The cooling air is supplied by a rotary piston blower and a special distributor containing a rotating disk with orifices for mass flow rate pulsation.

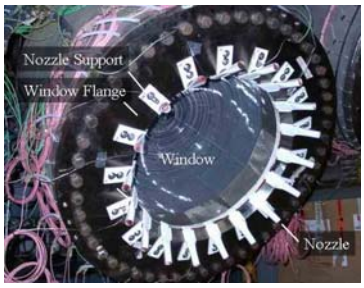

Fig. 30: Preinstalled nozzles on window flange of high-temperature receiver

Fig. 31 shows simulated and measured temperatures on the window outside. The asymmetric, pulsating air-jet cooling operated at a nozzle Reynolds number of Re=41,500. An air outlet temperature of 967°C was reached and a mean absorber temperature of 1014°C was measured. The window temperature was kept below ~800°C. Measurement and simulation are in good agreement (Reason for column pattern in measurement see paper [3]).

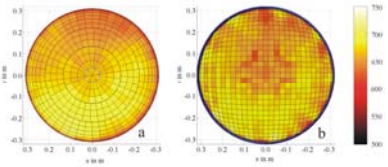

Fig. 31: Simulated (a) and measured (b) temperatures on the window outside (front view)

Fig. 32 shows simulated and measured temperature over time at a point on the window outside. The cycle duration of the well-cooled region was about 21 s.

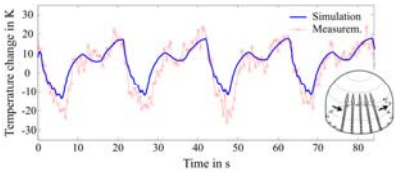

Fig. 32: Simulated and measured temperature response at a point on the window outside

The solar tests verified that the external air-jet window cooling with mass rate pulsation provides sufficient and homogeneous cooling on the receiver window. Integration in a high-temperature receiver is easy and cooling is reliable. The transmission of solar radiation is not affected by the window cooling installations. Investment, operation, and maintenance costs are low. By simply adapting the cooling mass flow through the nozzles, the cooling power can be adjusted to the actual operating conditions of the receiver. With the external window cooling, air outlet temperatures over 1000°C can be reached, maintaining window temperatures below 800°C.

The solar tests verified the solar radiation model and the thermodynamic receiver model successfully. Moreover, the measurements with activated window cooling are represented with high accuracy by the developed models and correlations.

You may also see paper [3] for more details.